2018 European Control Conference (ECC)
June 12-15, 2018. Limassol, Cyprus

In-domain energy control of the sine-Gordon model

Yury V. Orlov[1], Alexander L. Fradkov[2], and Boris Andrievsky[2]

Abstract— **The primary concern of the present investigation is the energy control of the nonlinear sine-Gordon model driven by several in-domain actuators. The speed-gradient method that has corroborated its utility for the sine-Gordon model, controlled through the manipulable parameters of the external electrical field and boundary actuation, is now generalized to the in-domain actuation, aiming to pump/dissipate the energy of the model to a desired level. Capabilities of the method are illustrated in numerical simulations.**

Index Terms— **sine-Gordon equation, energy control, speed-gradient**

I. INTRODUCTION

The sine-Gordon equation has become one of important models of modern nonlinear physics during the recent years [1]. On one hand it provides a number of interesting examples for complex nonlinear behavior such as solitons, kinks, antikinks, breathers, etc. On the other hand it presents the basis for modeling various physical processes in nonlinear optics (propagation of an optical pulse in fibre waveguide [2]), in mechanics (transition from a static to a dynamic frictional regime [3]), etc.

It is not surprising that there were attempts to control the solutions of sine-Gordon models. In the first publications [4]–[6], however only stabilization problem was studied. The energy control problem was formulated in [7] and the speed-gradient based control algorithm was then proposed.

Later on [8], the importance of the energy control was carried out in the simulation study of travelling waves. Distributed and spatially invariant energy control algorithms were rigorously studied in [9]. Both algorithms revealed, however, certain limitations. Being hardly feasible in practice, the distributed control algorithm called for further investigation on its implementation whereas the spatially invariant algorithm suffered from the generation of a nontrivial invariant manifold, possessing parasitic dynamics of distinct energy levels rather than the one to be imposed on the closed-loop system.

The present work makes a step beyond the aforementioned papers by admitting the use of in-domain actuators. Such actuators, being inserted within the plant domain with small spatial distributions, are yet feasible in practice whereas their combination is shown to yield more opportunities for reducing the invariant manifold with parasitic dynamics of undesirable energy levels. The speed gradient method is now reworked for the sine-Gordon model with in-domain actuators, and its effectiveness is additionally supported by numerical simulations.

The rest of the paper is outlined as follows. In Sec. II, the energy control problem is stated for the sine-Gordon model with in-domain actuators. Section III presents a speed gradient solution to the problem of interest. In Sec. IV, theoretical results are illustrated in numerical simulations. Finally, Sec. V accumulates some conclusions.

Notation

Standard notation is used throughout. Particularly, $x_t = \dfrac{\partial x}{\partial t}$, $x_{tt} = \dfrac{\partial^2 x}{\partial t^2}$, $x_r = \dfrac{\partial x}{\partial r}$, $x_{rt} = \dfrac{\partial^2 x}{\partial r \partial t}$, $x_{rr} = \dfrac{\partial^2 x}{\partial r^2}$ stand for the corresponding partial derivatives of $x(r,t) : \mathbb{R}^2 \to \mathbb{R}$. Also recall that the Sobolev space $H^l(a,b)$ with a natural index l consists of l times weakly differentiable functions $x(r) : \mathbb{R} \to \mathbb{R}$, which are defined on the domain $(a,b) \subset \mathbb{R}$ and whose norm is given by

$$\|x(\cdot)\|_{H^l(a,b)} = \sqrt{\sum_{j=1}^{l} \int_a^b \left(\frac{\partial^j x}{\partial r^j}\right)^2 dr}.$$

By default, $H^0(a,b) = L_2(a,b)$ and $H^l(0,1) = H^l$.

II. PROBLEM STATEMENT

The benchmark model of interest is a dissipation-free sine-Gordon system (of unit inertia) governed by

$$x_{tt} = kx_{rr} - F_0 \sin x + u(r,t),\ t \geq 0,\ 0 \leq r \leq 1 \qquad (1)$$

where t is the time instant, $r \in [0,1]$ is the scalar spatial variable, $x = x(\cdot,t)$ is the instant state of the system, the parameter k is the elasticity of the system, F_0 stands for the external electrical field, $u(r,t)$ is for the manipulable input. In contrast to [9], the electrical field is no longer actuated by an external force, and F_0 represents the permanent basis level of the field.

Throughout, the available in-domain actuation

$$u(r,t) = \sum_{i=1}^{M} u_i(t)\mathbb{I}_i(r) \qquad (2)$$

is pre-specified with the indicator functions

*This work was partially supported by the Government of Russian Federation (grant No 074-U01). The stability analysis (Section III-B) was performed in the IPME RAS and supported by the Russian Science Foundation (grant No 14-29-00142).

[1]Yury V. Orlov is with Department of Electronics and Telecomunications Mexican Scientific Research and Advanced Studies Center of Ensenada, Carretera Tijuana-Ensenada, B.C. 22860, México and ITMO University, Saint Petersburg, Russia yorlov@cicese.mx

[2]Alexander L. Fradkov and Boris Andrievsky are with the Institute for Problems of Mechanical Engineering of RAS, 61 Bolshoy prospekt, V.O., 199178, Saint Petersburg; Saint Petersburg State University; ITMO University, Saint Petersburg, Russia fradkov@mail.ru, boris.andrievsky@gmail.com

$$\mathbb{I}_i(r) = \begin{cases} 1 & \text{if } \ r \in (r_i, r_i + h_i), \quad i = 1, \dots M, \\ 0 & \text{otherwise}, \end{cases} \tag{3}$$

of disjoint subdomains $(r_i, r_i + h_i) \subset [0,1]$, of some lengths $h_i > 0$, and it is constituted by M actuators $u_i(t)$, acting over the corresponding subdomains (r_i, r_{i+1}). As far as the closures $[r_i, r_i + h_i]$ of the disjoint subdomains cover the entire domain, i.e., $\cap_{i=1}^{M} [r_i, r_i + h_i] = [0,1]$ and the maximal length $h_{max} = max_{1 \le i \le M} h_i$ approaches zero as $M \to \infty$, the in-domain actuation approaches the distributed one and can be viewed as an appropriate approximation of a distributed control action by means of MEMS (micro-electromechanical systems) array [10]. Another interpretation of the in-domain actuation is inspired from the case where $M = 1$ and the controlled input $u_1(t)$ is inversely proportional to the length h of the actuation subdomain $(1-h, 1)$ with an infinitesimal h. This case matches to the boundary actuation $u(r,t) = \delta(r-1)u(t)$, studied in [11] for the sine-Gordon energy control under the Dirichlet boundary condition at the left end and Neumann boundary condition at the right end. The present investigation rules out the boundary actuation and for certainty, it focuses on the sine-Gordon model with fixed ends, which is why the PDE (1) is subsequently accompanied with the Dirichlet boundary conditions

$$x(0,t) = 0, \ x(1,t) = 0. \tag{4}$$

The above system belongs to a class of nonlinear wave PDEs, and it can be viewed as a continuum model of diffusively coupled oscillators (e.g. pendulums, magnetic domains liquid crystals), whose instant state $x(r,t)$ at t represents the deflection angle of the oscillator, located at r. Thus interpreted, the sine-Gordon model is fully actuated, if controlled by the distributed signal $u(r,t)$, and it becomes underactuated when the finite-dimensional in-domain actuation (2) is applied. Remarkably, the infinite-dimensional system (1), (4), driven by the finite number of the in-domain actuators (2), is of *infinite underactuation degree*.

The control objective is to pump or dissipate the energy

$$E(x, x_t) = \frac{1}{2} \int_0^1 \Big[x_t^2 + k x_r^2 + 2F_0 \big(1 - \cos x\big) \Big] \, dr \tag{5}$$

of the sine-Gordon system (1), (2), (4) to a prespecified level $E_* \ge 0$ for guaranteing the limiting relation

$$\lim_{t \to \infty} E(x(\cdot,t), x_t(\cdot,t)) = E_* \tag{6}$$

on the solutions $x(r,t)$ of the closed-loop sine-Gordon model (1), (4).

Clearly, the energy control concept (6) can be reformulated in terms of the exact controllability once a specific generalized coordinate among the continuum of the oscillators is to be regulated to the desired energy level while the others are to be stabilized around the origin. It should be noted, however, that the proposed interpretation does not trivialize the energy control problem because the exact controllability of the nonlinear sine-Gordon boundary-value problem represents a real challenge under the infinite underactuation degree.

III. ENERGY CONTROL SYNTHESIS

Introduce the *goal function* as

$$V(t) = \frac{1}{2} \big(E(t) - E_* \big)^2. \tag{7}$$

Following the speed-gradient design procedure [7], [12], let us compute the time derivative of the goal function along the system (1), (4) trajectories, provisionally assuming that $u(r,t)$ is constant on t. Thus one derives

$$\begin{aligned} \dot V = \frac{dV}{dt} &= \big(E(t) - E_* \big) \int_0^1 \left(x_t \cdot x_{tt} - k x_{rr} \cdot x_t + F_0 \sin x \cdot x_t \right) dr \\ &= \big(E(t) - E_* \big) \int_0^1 u(r, \cdot) \cdot x_t \, dr. \end{aligned} \tag{8}$$

Let the control action in the form of a finite number in-domain actuators (2) be taken. Then $\dot V$ reads as

$$\dot V = \big(E(t) - E_* \big) \sum_{i=1}^{M} \left(u_i(\cdot) \int_{r_i}^{r_i + h_i} x_t \, dr \right). \tag{9}$$

As the second step of the speed-gradient procedure, one should derive the gradient $\nabla_u \dot V \in \mathbb{R}^M$ of the resulting expression of $\dot V$ with respect to the control components $u_i(t)$, $i = 1, \dots, M$, thus arriving at

$$\nabla_u \dot V = \big(E(t) - E_* \big) \begin{bmatrix} \int\limits_{r_1}^{r_1 + h_1} x_t \, dr & \dots & \int\limits_{r_i}^{r_i + h_i} x_t \, dr \end{bmatrix}^{\mathrm{T}}. \tag{10}$$

The third step of the speed-gradient procedure is to pick up a certain function $\psi(x,u,t)$ which forms an acute angle with $\nabla_u \dot V$, i.e. satisfies an inequality $\psi(x,u,t)^{\mathrm{T}} \nabla_u \dot V \ge 0$. Let

$$\psi(x,u,t) = \operatorname{sign} \big(E(t) - E_* \big) \begin{bmatrix} \int\limits_{r_1}^{r_1 + h_1} x_t \, dr & \dots & \int\limits_{r_i}^{r_i + h_i} x_t \, dr \end{bmatrix}^{\mathrm{T}}$$

be chosen. Then in accordance with the speed-gradient design procedure, the control action is taken as $u(r,t) = -\Gamma \psi(x,u,t)$, where $\Gamma = \Gamma^{\mathrm{T}} > 0$ is the matrix design parameter. Setting $\Gamma = \operatorname{diag}\{\gamma_1, \dots, \gamma_M\}$, with positive entries γ_i, one finally obtains the in-domain actuation (2) in the form

$$u_i(t) = -\gamma_i \operatorname{sign} \big(E(t) - E_* \big) \int_{r_i}^{r_i + h_i} x_t \, dr, \quad i = 1, \dots, M. \tag{11}$$

For ensuring that the time derivative (9) of the goal function (7) is non-positive it suffices to substitute (11) into (8) and verify that

$$\frac{dV}{dt} = -\big| E(t) - E_* \big| \sum_{i=1}^{M} \gamma_i \Big(\int_{r_i}^{r_i + h_i} x_t \, dr \Big)^2 \le 0. \tag{12}$$

Thus, if the sine-Gordon model is enforced by the discontinuous actuation (11) it has a tendency to meet the control objective (6).

A. Closed-loop Sliding Mode Dynamics

It should be pointed out that due to (12), the closed-loop system cannot escape from the discontinuity manifold

$$\mathbb{S} = \{(s,s_t) \in H^1 \times H^0 : E(s,s_t) - E_* = 0\} \tag{13}$$

where it evolves in the sliding mode [13]. Although the finite time attractiveness of manifold (13) is not guaranteed, the stability analysis of the closed-loop system is however developable regardless of this feature.

To describe potential sliding modes on the discontinuity manifold (13) a continuous equivalent control value u_{eq}, cf. [13], driving the system along (13), is to be substituted into the plant equation (1) for $u(r,t)$. The interested reader may refer to [14] for details of the sliding mode description in the PDE setting. For the purpose of deriving the equivalent control value, let us denote

$$S(s,s_t) = E(s,s_t) - E_* = 0 \tag{14}$$

and differentiate the sliding mode relation $S = 0$ on the trajectories of the closed-loop system (1)–(4) and determine the equivalent control value $\mathrm{sign}_{eq} S(s,s_t)$ that satisfies the resulting relation

$$\dot{S} = \frac{dE}{dt} = \int_0^1 (x_t \cdot x_{tt} + x_r \cdot x_{rt} + F_0 \sin x \cdot x_t)\, dr = \\ -\mathrm{sign}_{eq} S(s,s_t) \sum_{i=1}^{M} \gamma_i \Big(\int_{r_i}^{r_1+h_i} x_t\, dr \Big)^2 = 0. \tag{15}$$

Regardless of whether $\int_{r_i}^{r_1+h_i} x_t\, dr = 0$ for all $i = 1,\dots,M$ or $\mathrm{sign}_{eq} S(s,s_t) = 0$, it follows that

$$u_{eq} = -\mathrm{sign}_{eq} S(s,s_t) \Big(\sum_{i=1}^{M} \gamma_i \int_{r_i}^{r_i+h_i} x_t\, dr \Big) = 0 \tag{16}$$

on the discontinuity manifold (13). Hence, the boundary-value problem, governing the sliding modes of the closed-loop system (1)–(4), driven by the discontinuous controller (11) along the pre-specified energy level (13), is naturally given by the open-loop ($u \equiv 0$) sine-Gordon model (1), (4).

B. Well-posedness of the Closed-loop System and its Stability Analysis

The closed-loop boundary-value problem (1)–(4), (11) is subsequently studied in the state space $H^1 \times H^0$. For a technical reason of ensuring a sufficiently smooth mild solution of the boundary-value problem (BVP) (1), (4) to exist in an appropriate Sobolev space, a non-zero initial state

$$x(0,r) = x^0(r) \in H^3,\ x_t(0,r) = x^1(r) \in H^2 \tag{17}$$

is assumed to be of class $H^3 \times H^2$. For later use, let us introduce the manifold

$$W = \Big\{ (w,w_t) \in H^1 \times H^0 : \\ \Big(E(t) - E_*\Big) \Big[\sum_{i=1}^{M} \Big| \int_{r_i}^{r_i+h_i} x_t\, dr \Big| \Big] = 0 \Big\} \tag{18}$$

where the time derivative (12) of the goal function (7) is nullified. The following result is then in force.

Theorem 1: Let the sine-Gordon model (1)–(4) be initialized within $H^3 \times H^2$ and let it be driven by the state feedback (11). Then given an arbitrary non-zero initial state (17), there exists a unique mild solution $x(r,t)$ of the closed-loop system (1)–(4), (11) beyond the discontinuity manifold (13) which evolves along this set in the sliding mode, governed by the open-loop boundary-value problem (1)–(4) with $u \equiv 0$. Furthermore, such a solution is globally defined and uniformly bounded in $H^2 \times H^1$, and its deviation $\inf_{\mathbf{z} \in Z} \|(x(\cdot,t), x_t(\cdot,t)) - (z,z_t)\|_{H^1 \times H^0}$ from the maximal invariance subset Z of manifold (18) converges to zero as $t \to \infty$. In addition, the control components (11) remain uniformly bounded for all $t \in [0,\infty)$ and their maximal magnitudes approaches zero

$$\sup_{t \in [0,\infty)} |u_i(t))| \to 0 \tag{19}$$

as the controller gains $\gamma_i, i = 1,\dots,M$ approach zero.

Proof is brought up into several steps.

1. A unique local solution of the closed-loop system is shown to exist by following the line of reasoning used in the proof of [9, Theorem 4.1].

2. The closed-loop solutions are uniformly bounded in $H^1 \times H^0$. Indeed, due to (12), the energy function (5) admits an *a priori* estimate

$$V(t) \le V(0) \quad \forall t \in [0,\infty). \tag{20}$$

Hence, an arbitrary local solution of the closed-loop system (1)–(4), (11) admits an *a priori* estimate in $H^1 \times H^0$, too. Thus, such a solution is continuously extendible to the entire semi-infinite time axis $[0,\infty)$ because otherwise, its norm would escape to infinity in finite time what is impossible due to (20). As a matter of fact, starting from a finite time instant, the global solution may evolve in the sliding mode, governed by the open-loop ($u \equiv 0$) sine-Gordon model (1)–(4) along the discontinuity manifold (14) (for description of potential closed-loop sliding modes, see Subsection III-A).

3. The uniform boundedness of the control signal and its negligibility is established as follows. Since (20) ensures that the energy function (5) is uniformly bounded, regardless of whichever control gain $\gamma > 0$ is chosen. Thus, the control signal (11) is uniformly bounded, too, and convergence (19) holds.

3. Asymptotic convergence to the maximal invariant subset Z of manifold (18) is demonstrated by applying the PDE-flavored invariance principle [15]. As in the proof of [9, Theorem 4.2], the closed-loop sine-Gordon model (1)–(4), (11) determines a dynamic system on the Hilbert space $H^1 \times H^0$ with all mild solutions bounded and precompact. Hence, the infinite-dimensional version of the invariance principle from [15] is applicable to the closed-loop sine-Gordon model, and by applying this principle, all solutions of (1)–(4), (11) are guaranteed to approach the maximal invariant subset of manifold (18. This completes the proof of Theorem 1.

IV. NUMERICAL RESULTS

A. Computational Algorithm

In the numerical study, the PDE (1) is discretized in the spatial variable $r \in \mathbb{R}^1$ by uniformly splitting the segment $[0,1]$ into N sub-intervals. The *discretization step* ν is introduced as $\nu = 1/N$. The resulting system of $N-1$ ordinary differential equations (ODEs) of the second order are then numerically solved over a time interval $[0,T]$ by applying the medium order variable step Runge-Kutta Method [16], performed with the standard MATLAB routine *ode45*.

At the discretization nodes $r_i = i \cdot \nu$, $i = 1,\ldots,N-1$, the second-order spatial derivatives of $x(r,t)$ are approximately computed as

$$x_{rr}(r_i,t) = \frac{x(r_{i+1},t) - 2x(r_i,t) + x(r_{i-1},t)}{\nu^2}. \qquad (21)$$

The boundary values $x(r_0,t) = x(r_1,t)$, $x(r_N,t) = x(r_{N-1},t)$ are specified according to the Dirichlet boundary conditions (4), thereby yielding the following values $x(r_0,t) = x(r_N,t) = 0$ at the boundaries. The remaining discrete values $x(r_1,t)$, $\ldots$, $x(r_{N-1},t)$ are found by solving $(N-1)$ ODEs numerically.

To numerically find the values of definite integrals in (11), the MATLAB standard routine *trapz* of the trapezoidal numerical integration are used.

B. Simulation Results

In the simulations of the closed-loop boundary-value problem (1), (4), (11), the control gains were set to $\gamma_i = 5/h$ and the desired energy levels were taken as $E_* = 0$ (energy dissipating) and $E_* = 10$ (energy pumping) for different simulation runs. In addition, the initial states were prespecified in the form

$$x(0,r) = A\big(1 - \cos(2\pi r)\big)^7, \quad x_t(0,r) = 0 \qquad (22)$$

with a certain "magnitude" parameter A. A reasonably high number $N = 2500$ was selected for the PDEs (1) to discretize the spatial variable r and duration of the computation time T was confined to 3. Two cases of the actuation domain partition were examined and compared. The first one was an "integral" control, where $u(r,t)$ did not depend on r and thereby, the same action $u(t)$ was applied to all points $r \in [0,1]$. This case corresponded to $r_1 = 1$ and $h_1 = 1$. The second case with $M = 10$ leaded to the piecewise constant in r function $u(r,t)$ having 10 intervals of constancy with lengths $h_i = 0.1$ and left ends $r_i = 0.1 \cdot (i-1)$, $i = 1,\ldots,10$. For the simulations, model (1) parameters were specified to $k = 0.12$, F_0=25.

At the first series of simulation runs, parameter A in the initial conditions (22) was set to $A = 10^{-3}$, which corresponded to a lower initial energy level than the desired one $E_* = 10$. Figures 1–3 are for the case of $M = 1$ to illustrate the closed-loop system (1), (4), (11) performance by means of the time histories of the system energy $E(t)$ and of spatiotemporal graph of $x(r,t)$. Respectively, Figs. 4–6 are for the case of $M = 10$. As seen from Figs. 1, 4 in both cases, the energy reaches the prescribed value $E_* = 10$ in finite time and after that, the sliding mode arises. For plotting Figs. 3, 6, equivalent control action $u_{\text{eq}}(r,t)$ was calculated by passing control $u(r,t)$ through the first-order low-pass filter with cutoff frequency 50 rad/s. One may observe that the transient time is a bit less for $M = 10$ compared to that of $M = 1$. An opposite situation appears in the energy dissipation case where $E_* = 0$. Just in case, the "integral" control action (with $M = 1$) does not ensure achievement of the control goal $E(t) \to E_*$ and the system trajectories converge to a certain manifold with energy $E \approx 14.8$, see Figs. 7–9. As seen from Figs. 10–12, in the case of $M = 10$, the control goal is achieved. Thus,the numerical results demonstrated that an "intergal" (uniformly distributed over the whole spatial interval $[0,1]$) control action with $M = 1$ may not suffice to lead to the control objective (6) and more in-domain actuators are required to avoid the invariance manifold $\dot{V} = 0$ with parasitic dynamics with non-desired energy levels.

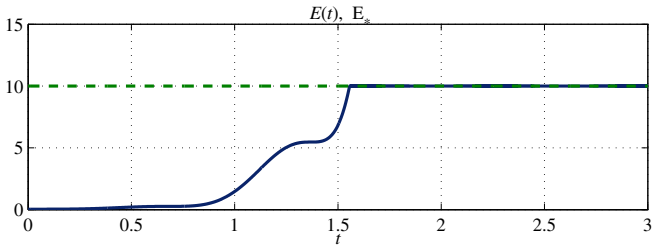

Fig. 1. Time history of energy $E(t)$. Case $M = 1$, $A_0 = 10^{-3}$, $E_* = 10$.

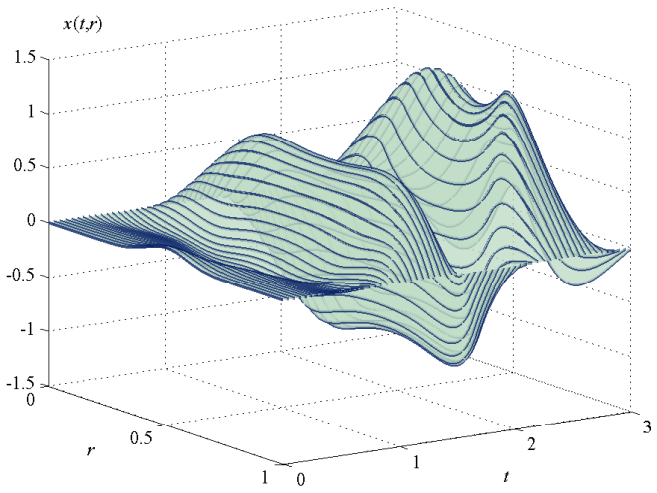

Fig. 2. Spatiotemporal graph of $x(r,t)$. Case $M = 1$, $A_0 = 10^{-3}$, $E_* = 10$.

V. CONCLUSIONS

The speed gradient method [7], which is long recognized as a powerful tool of the energy control of Lagrangian systems, and the sliding mode approach in the infinite-dimensional setting [14] are coupled together to develop the in-domain energy control of a nonlinear sine-Gordon model. In contrast to [9], [17], where controlling the energy of the sine-Gordon model was enforced by using the manipulable parameter (intensity) of the external electrical

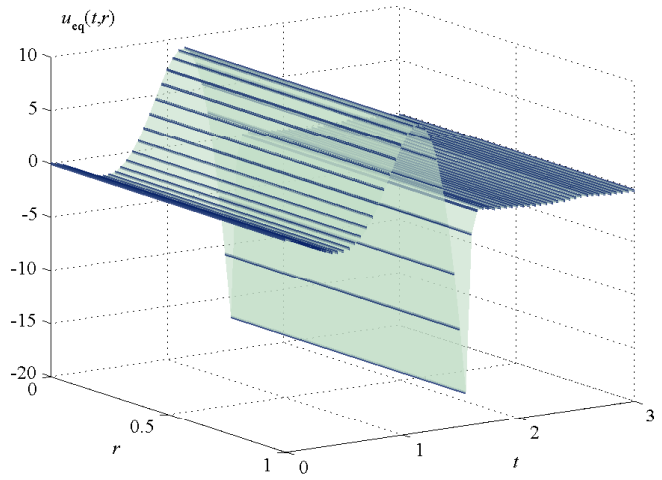

Fig. 3. Spatiotemporal graph of equivalent control $u_{\rm eq}(r,t)$. Case $M=1$, $A_0=10^{-3}$, $E_*=10$.

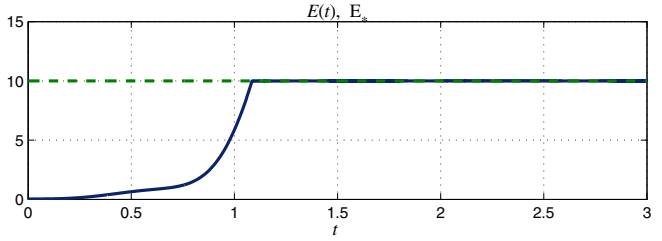

Fig. 4. Time history of energy $E(t)$. Case $M=10$, $A_0=10^{-3}$, $E_*=10$.

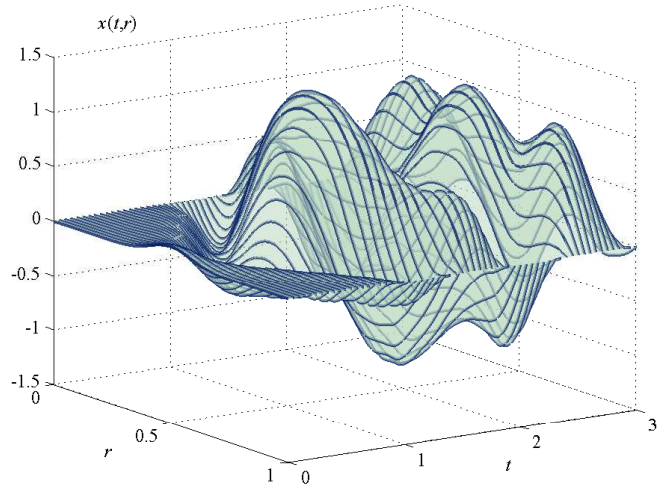

Fig. 5. Spatiotemporal graph of $x(r,t)$. Case $M=10$, $A_0=10^{-3}$, $E_*=10$.

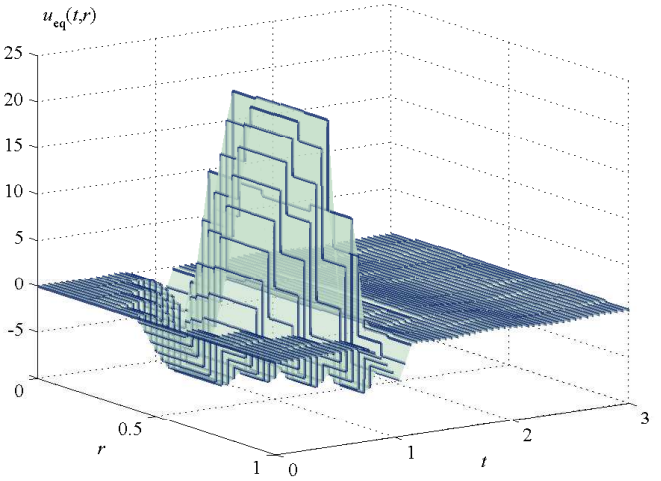

Fig. 6. Spatiotemporal graph of equivalent control $u_{\rm eq}(r,t)$. Case $M=10$, $A_0=10^{-3}$, $E_*=10$.

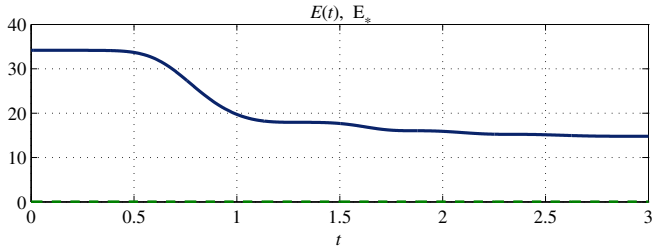

Fig. 7. Time history of energy $E(t)$. Case $M=1$, $A_0=0.05$, $E_*=0$.

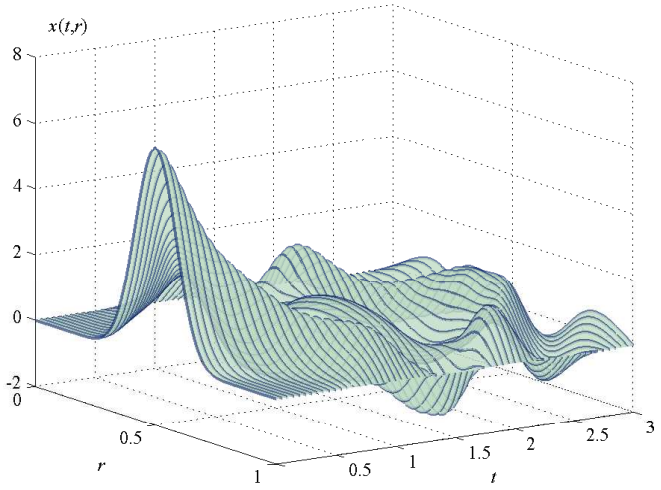

Fig. 8. Spatiotemporal graph of $x(r,t)$. Case $M=1$, $A_0=0.05$, $E_*=0$.

field and, respectively, by the boundary actuation, the present investigation calls for the first time to achieve the energy performance via the spatially-discretized actuation, located within the plant domain. Applying the speed gradient method to the problem in question yields the sliding mode in-domain regulator that ensures the well-posedness of the resulting closed-loop system as well as its desired energy level to be achieved under a broader class of the plant initial conditions than e.g., that numerically verified for the spatially uniform actuation. The proposed in-domain regulator is yet feasible in practice and it can be viewed as an appropriate approximation of the distributed actuation which is in general unrealistic in the implementation.

In the future research it is planned to expand the proposed in-domain control scheme to the problem of localization of nonlinear waves [18] in the sine-Gordon model.

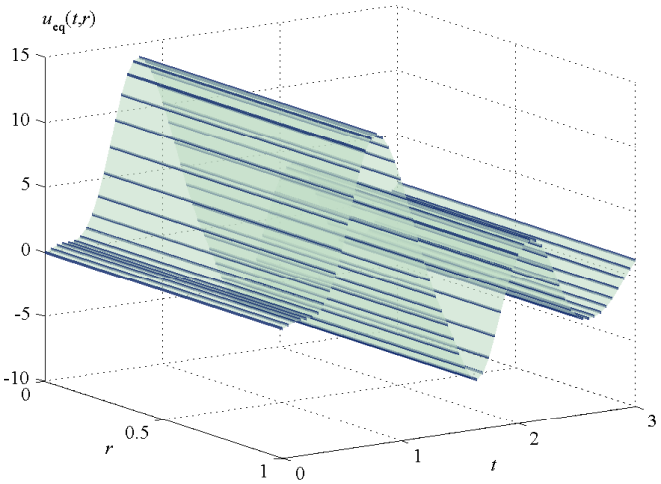

Fig. 9. Spatiotemporal graph of $u(r,t)$. Case $M = 1$, $A_0 = 0.05$, $E_* = 0$.

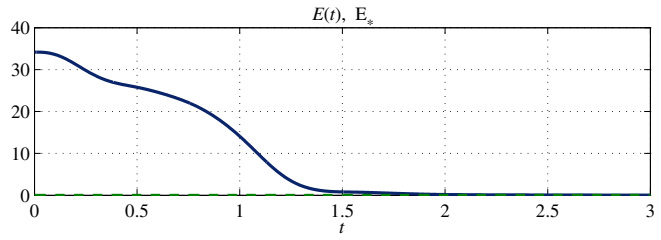

Fig. 10. Time history of energy $E(t)$. Case $M = 10$, $A_0 = 0.05$, $E_* = 0$.

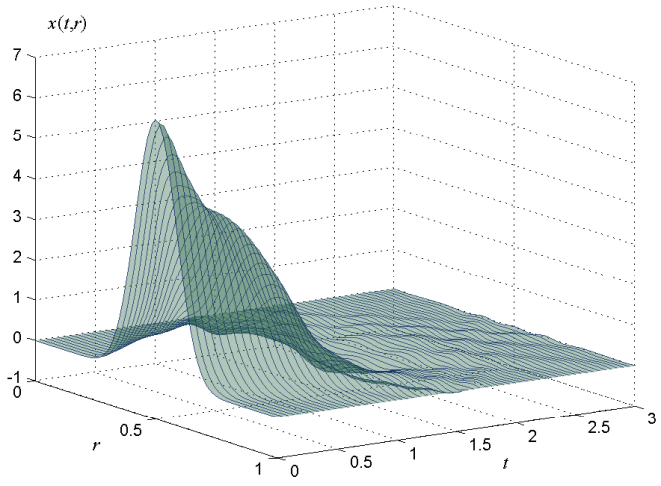

Fig. 11. Spatiotemporal graph of $x(r,t)$. Case $M = 10$, $A_0 = 0.05$, $E_* = 0$.

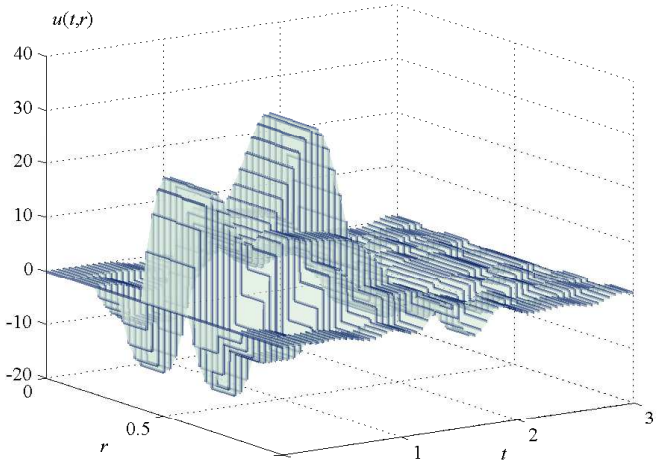

Fig. 12. Spatiotemporal graph of $u(r,t)$. Case $M = 10$, $A_0 = 0.05$, $E_* = 0$.

REFERENCES

[1] J. Cuevas-Maraver, P. Kevrekidis, and F. Williams, Eds., *The sine-Gordon Model and its Applications. From Pendula and Josephson Junctions to Gravity and High-energy Physics*. Springer-Verlag, 2014.

[2] Q. Zhou, M. Ekici, M. Mirzazadeh, and A. Sonmezoglu, "The investigation of soliton solutions of the coupled sine-gordon equation in nonlinear optics," *J. of Modern Optics*, vol. 64, no. 16, pp. 1677–1682, 2017.

[3] N. I. Gershenzon, G. Bambakidis, and T. E. Skinner, "Sine-Gordon modulation solutions: Application to macroscopic non-lubricant friction," *Physica D: Nonlinear Phenomena*, vol. 333, pp. 285–292, 2016.

[4] T. Kobayashi, "Boundary feedback stabilization of the sine-Gordon equation without velocity feedback," *J. of Sound and Vibration*, vol. 266, pp. 775–784, 2003.

[5] M. Petcu and R. Temam, "Control for the sine-Gordon equation," *ESAIM: Control, Optimisation and Calculus of Variations*, vol. 10, no. 4, pp. 553–573, 2004.

[6] T. Kobayashi, "Adaptive stabilization of the sine-gordon equation by boundary control," *Mathematical methods in the applied sciences*, vol. 27, no. 8, pp. 957–970, 2004.

[7] A. L. Fradkov, *Cybernetical Physics. From Control of Chaos to Quantum Control*. Springer, Feb. 2007.

[8] A. Porubov, A. Fradkov, and B. Andrievsky, "Feedback control for some solutions of the sine-Gordon equation," *Applied Mathematics and Computation*, vol. 269, pp. 17–22, 2015.

[9] Y. Orlov, A. Fradkov, and B. Andrievsky, "Energy control of distributed parameter systems via speed-gradient method: case study of string and sine-Gordon benchmark models," *Intern. J. of Control*, vol. 90, no. 11, pp. 2554–2566, 2017.

[10] B. Bamieh, F. Paganini, and M. Dahleh, "Distributed control of spatially-invariant systems," *IEEE Trans. Automat. Contr.*, vol. 47, pp. 1091–1107, 2002.

[11] M. Dolgopolik, A. Fradkov, and B. Andrievsky, "Boundary energy control of the sine-Gordon equation," *IFAC-PapersOnLine*, vol. 49, no. 14, pp. 148–153, 2016.

[12] A. L. Fradkov, I. V. Miroshnik, and V. O. Nikiforov, *Nonlinear and Adaptive Control of Complex Systems*. Dordrecht: Kluwer, 1999.

[13] V. Utkin, *Sliding modes in control and optimization*. Berlin: Springer-Verlag, 1992.

[14] Y. Orlov, *Discontinuous Systems – Lyapunov Analysis and Robust Synthesis under Uncertainty Conditions*. London: Springer-Verlag, 2009.

[15] J. A. Walker, *Dynamical systems and evolution equations*. New York: Plenum Press, 1980.

[16] J. R. Dormand and P. J. Prince, "A family of embedded Runge-Kutta formulae," *J. Comp. Appl. Math.*, vol. 6, pp. 19–26, Mar. 1980.

[17] M. Dolgopolik and A. Fradkov, "Nonsmooth and discontinuous speed-gradient algorithms," *Nonlinear Analysis: Hybrid Systems*, vol. 25, pp. 99–113, 2017.

[18] A. Porubov and B. Andrievsky, "Control methods for localization of nonlinear waves," *Philosophical Transactions of the Royal Society A: Mathematical, Physical and Engineering Sciences*, vol. 375, no. 2088, 2017.